Hindawi
Advances in Civil Engineering
Volume 2022, Article ID 6989122, 17 pages
https://doi.org/10.1155/2022/6989122

Research Article

Stability Analysis of the New Section in Raising the Existing Composite Wala Dam Using Finite Element Methods

Dima A. Husein Malkawi[1] **and Abdallah I. Husein Malkawi**[2]

[1]*Department of Civil and Environmental Engineering, German Jordanian University, Amman, Jordan*
[2]*Fahad Bin Sultan University, On Leave from Jordan University of Science and Technology, Tabuk, Saudi Arabia*

Correspondence should be addressed to Dima A. Husein Malkawi; dima.malkawi@gju.edu.jo

Received 26 April 2022; Revised 8 August 2022; Accepted 10 August 2022; Published 19 September 2022

Academic Editor: Wen-Da Wang

Jordan is a country with a population that increases steadily but is punctuated by waves of refugees. Henceforth, Jordan will be destabilized with prolonged and potential water shortages. With both climate and population changes, the nation needs to implement comprehensive reform. In many cases, raising the height of an existing dam would help reduce the gap between the sources and water demands. Consequently, the original Wala dam in Jordan with a capacity of 9.3 million cubic meters (MCM) was raised to achieve a capacity of 25 MCM. The Wala dam was raised uniquely and unusually, which raises concerns about its stability and safety. In this paper, a two-dimensional plane strain model was conducted using finite element modeling (FEM) on the Wala dam to investigate the stability conditions of the raised dam. Several material properties were used in this study. These properties are density, Poisson's ratio, elastic modulus, and friction angle. Stresses and deformations of the new section within the dam body, dam foundation, and an earthfill embankment are presented and compared with the original dam. Results showed that the stresses after raising the height of the dam body are below 1.5 MPa, and it is within the allowable range. Moreover, the stability analysis showed that the stresses and deformation are minimal and negligible. Also, no failure was observed or reported within the soil. Furthermore, a stability analysis of the slip surface of the new body of the dam structure using the finite element method is introduced. Two potential slip surfaces were examined, and a surface-to-surface contact element is modeled to simulate the slip surface. In addition, settlement field observations for 16 months are presented and discussed in this paper.

1. Introduction

Water resources play a vital role in the sustainability of social, economic, and environmental sectors in the world. They are the pivot around which the wheel of development and productivity turns. Adopting nonsustainable practices for water resources management will ultimately lead to the depletion of these resources.

Jordan is considered a part of an arid and semiarid region of the Middle East, where its natural water resources are limited and more than 80% of its land is desert. Currently, Jordan is considered the fourth country in the world with severe water scarcity and facing high water demand problems, especially with 92% evaporation rates [1–3]. The exacerbated water scarcity in Jordan has led to the creation of difficult living conditions. Since the 1980s, the Ministry of Water and Irrigation (MWI) embarked on practical steps to reduce the depletion of water resources, by maintaining and sustaining the current water resources. Jordan's infrastructure is under immense pressure due to water scarcity, high unemployment rates, and the excessive influx of refugees.

In Jordan, dams (e.g., King Talal, Karameh, Kafrein, Mujib, Tannur, Wala dam) are considered the primary source of water with a capacity of 336 MCM as they store water from the surface runoff. In general, there are several types of dams that are constructed for water storage around the world (e.g., embankment dams, RCC dams, concrete dams); the main difference between those types is how they are designed. Hitherto, the stability of dams and their

foundations has always been a major design consideration. As with most engineering structures, dams may fail due to various reasons. For instance, dams may be prone to failure when seepage or induced stresses (either tension or compression) exceed the allowable limit.

There is a growing body of literature that focuses on investigating the stability of dams using finite element methods, for example, [1, 4–7]. However, there has been no detailed analysis done on investigating the expected behavior (deformation and stresses) of raising the composite dams' wall (e.g., Wala dam). This study developed a two-dimensional plane strain model to investigate the stability, stress distribution, and settlement of the Wala dam's newly constructed concrete wall. It critically compares the results of the stress distribution and deformations between the original section and the newly raised concrete section of the dam. Besides, field monitoring of the dam's settlement was conducted over a 16-month period using leveling surveys devices and joint meters that were placed at different locations of the dam's wall. Also, this study provides the needed and necessary knowledge about raising the dam's walls. As a result, it is recommended that MWI utilized the developed procedure to safely increase the dams' wall to accommodate the increased water demand.

2. Background

2.1. Dam Engineering. Like all fluids, water flows from areas of high pressure to low pressure. Dams are structures that essentially separate those two conditions [6]. This prime circumstance induces flow, whether through the dam itself or underneath through its foundation, thus reducing the dam capacity and affecting its operational life [8]. As far as infrastructures, dams are considered fairly risky. Depending on the size of the structure, the failure of a dam can be catastrophic. In fact, some of the worst human-caused disasters in history have been failures of dams. For this reason, it is often required to study and investigate dams' stability due to any structural changes [9].

This research seeks to investigate the stability of dams after raising the height of a dam's wall using a two-dimensional plane strain model, more specifically the Wala dam in Jordan. Understanding the link between raising the dam's wall and its stability will help engineers, practitioners, and stakeholders to better facilitate the limited resources and meet the increased water demand. However, the nature of this behavior remains largely unexamined as there has been little quantitative analysis and numerical modeling previously published.

Globally, with the increasing water demands and limited resources, difficulties in finding appropriate sites for constructing new dams resulted in more sustainable solutions such as raising the height of existing dams [10]. Several dams (e.g., gravity dams, arch dams, etc.) have been raised around the world over the years such as the Guri dam in Venezuela and the Kuroda dam in Japan [29] and [11–13]. The Guri dam was built to a height of 110 m and raised later to a height of 162 m in 1973. To determine the shape of the newly added structure, Chavarri, et al. studied the Guri dam stability and conducted stress analysis under several combinations of loading for the two stages [11]. That is, the newly added structure will meet the engineering requirements to avoid any structural failure in the dam's body or its foundation. On the other hand, the Kuroda dam was built to a height of 150 m and raised later by 10.2 m to increase the capacity of the reservoirs. Both dams, using experimental and numerical studies, were found to be stable.

Furthermore, the Gibraltar dam is a concrete arch dam that was built in 1920 to a height of 59.3 m and raised by 12 m in 1966. A stability analysis was conducted that showed the stresses developed under the dam would be higher than the allowable tensile strength of the concrete. Therefore, the dam was strengthened and raised by adding roller-compacted concrete gravity sections against the downstream face of the dam [10, 14]. In addition, the Bockhartsee dam located in Austria is a rockfill dam raised using a concrete wall of a 9 m height placed on the crest of the dam [3, 15]. Tschernutter et al. analyzed the dam using numerical analysis with different soil models and compared the result of the numerical analysis to the field monitoring data [3]. It was reported that unexpected settlements would occur. Also, it was found that only the top third of the downstream retaining wall backfilling mainly influences the original dam and produces those settlements.

In Jordan, to meet the country's increasing water demands, several dams' heights have been raised (e.g., King Talal Dam and the Wala dam). According to Haddadin, the King Talal Dam located in the hills of northern Jordan was built in 1978 to a height of 92.5 m and raised by 13.5 m in 1984 [16, 17]. The recently raised Wala dam, which is a composite dam (both RCC and earthfill embankment dam) located in the Madaba region in Jordan, is the main focus of this paper and will be discussed in detail in the following sections.

2.2. Stress-Deformation Analysis of Reinforced Dams. Recent years have seen renewed interest in studying the dam's stress-deformation behavior. However, there has been no detailed analysis done on investigating the expected behavior (deformation and stresses) of raising the composite dams' wall (e.g., Wala dam). Finite element modeling is among the most widely used numerical techniques to study and analyze this behavior.

Numerical techniques (e.g., FEM and limit equilibrium method) are fast becoming key instruments in studying structural failures (e.g., dams). Chen et al. reported that challenging engineering tasks can be analyzed systematically and comprehensively by integrating numerical techniques and simulations with testing models [18]. For instance, a two-dimensional FEM was performed by Liu et al. 2016 to study and analyze a rockfill dam with clay core that was constructed on a deep overburden layer along with some stress-strain behaviors affecting factors of the cut wall [19].

Relatively, three-dimensional finite element modeling is one of the most frequently numerical techniques used. This technique was used with the Duncan-Chang E-ν model to calculate and simulate dams' stress-strain deformation. For

instance, Cherif et al. (2021) and Chu, F. Y. (2014) studied the stress-strain deformation of a core rockfill dam that is placed in a narrow canyon [24] and [8, 20]. The three-dimensional finite element modeling showed that the stresses and deformations are allowable.

There is an urgent need to address the safety of raising the dams' height. For example, Toumi and Remini as well as Wong and Yu studied the stress-strain characteristics using the FEM and Duncan-Zhang E-B nonlinear elastic hyperbolic model of the Panshitou reservoir's high concrete face rockfill dam [30] [9, 21]. The results showed that this type of analysis would provide practitioners and engineers with a theoretical understanding of the dam's safety, especially for the dam's construction and operation.

2.3. Description of the Wala Dam

2.3.1. Location and Dimension. The Wala dam, owned by the Jordan valley authority, is located in the Madaba region about 40 km south of the Jordanian capital "Amman" as seen in Figure 1 and is mainly used to store runoff water for the purpose of water supply and irrigation. The dam type is a recharge dam; the stored water is used for aquifer recharge through a series of recharge wells that are constructed between 1999 and 2002. This dam is a hybrid dam composed of a central roller-compacted concrete (RCC) gravity dam and earthfill embankment at the abutments (see Figure 2 and Figure 3) [22, 23]. The original dam has a maximum height of 52 m above the foundation level, a dam crest length of 380 m with a reservoir capacity of 9.3 MCM [24]. Afterward, the dam was raised by 16 m between 2017 and 2020, making the new section 67 m above the foundation level, raising the reservoir capacity to approximately 25 MCM. The spillway is raised using RCC and conventional concrete (CVC) with an upstream face inclined at 0.2H/1V and a downstream face inclined at 0.7H/1V. The height of the concrete wall is approximately 20 m; 3.8 m for the upstream side is embedded within the core of the dam forming the foundation of the wall. Moreover, as shown in Figure 3, about 9 m are covered by the roller-compacted rock fill material for the downstream side. The wall of the wing embankments is of a unique design due to the complexity of its construction. Therefore, the wing embankments were raised with a concrete retaining structure at the dam crest and rockfill ballast at the downstream side, which is similar to the design of the Bockhartsee dam located in Austria. However, the Bockhartsee dam has a concrete core, whereas the Wala dam has a clay material core (RCC with earthfill abutments).

2.4. Geology of the Site. The geology of the site is dominated by 600 m thick Cretaceous sediments of Cretaceous age; Figure 4 shows the formation of the overlying sediments around the dam site. In this figure, the Wadi as Sir Limestone (WSL) consists mainly of limestone and dolomite of the Turonian stage. Also, Wadi Umm Ghudran (WG) formations (~85 m thick) make the dam's foundation and the reservoir and can be subdivided into three zones: (a) the Mujib Chalk member forms the foundation's dam with a high modulus of elasticity, comprised well-lithified carbonate mudstone and sandstone, and (b) the Tafilah member (~60 m thick) comprises different types of rocks (e.g., dolomite, limestone, mudrocks, and porcelanite). A high plastic clay layer of about 15 to 20 cm thick exists within the lower Tafilah member and the Mujib Chalk member, on both sides of the banks. (c) The Dhiban Chalk consists mainly of chalk marl composition that has a high sensitivity to erosion. Finally, the Amman Silicified Limestone (ASL), these formations (~75 m thick) are essentially a bedded chert and limestone positioned above the dam foundation [25].

The Wala dam was designed as a hybrid dam due to the geological conditions of the site, where the Upper Tafila and Dhiban Chalk formations were not capable of supporting an RCC dam. That is due to (a) the low modulus elasticity of the Upper Tafila (less than 1.0 GPa), (b) the high sensitivity to erosion, and (c) the high permeability of the Dhiban formation, whereas the Mujib Chalk forms the dam's foundation with a modulus of elasticity higher than 9 GPa [24]. As a result, the ends of the dam were built as an earthfill dam with an RCC at the center as shown in Figure 4.

2.5. Material Properties. In this study, several material properties were used to investigate the stability of the newly constructed Wala dam section. These properties are density, Poisson's ratio, elastic modulus, and friction angle; detailed information are summarized in Table 1. For the purpose of this study, the shear strength parameters have been adopted based on the Mohr–Coulomb linear law of failure that is based on laboratory and field testing carried out at the laboratories of the Jordan Valley Authority [17, 27] and [23, 26, 27].

Generally, compressive strength of 16 MPa for RCC (age 365 days) should be maintained. Based on Hadadin, the true tensile strength is found to be about 7% to 9% of the compressive strength [7]. Therefore, for the Wala dam, the required design tensile strength should be maintained below 1.5 MPa.

3. Finite Element Modeling

In this study, the ANSYS Mechanical Finite Element Analysis (FEA) Software for Structural Engineering was utilized to conduct the numerical calculations and analysis. This software is one of the widely used simulation software used for engineering simulations. In this work, this software was used to accurately analyze, simulate, and model the stress and deformations in the Wala dam with the newly constructed wall. The finite element models are meshed using the PLANE182 element type available in the ANSYS element library. The element has eight nodes with three degrees of freedom at each node (see Figure 5).

The dam was modeled as a two-dimensional plane strain model. This means that the condition for which the strains perpendicular to the plane of the analysis is maintained at zero. In this study, all materials are considered homogeneous with linear elastic behavior, and the foundation is uniform and homogeneous.

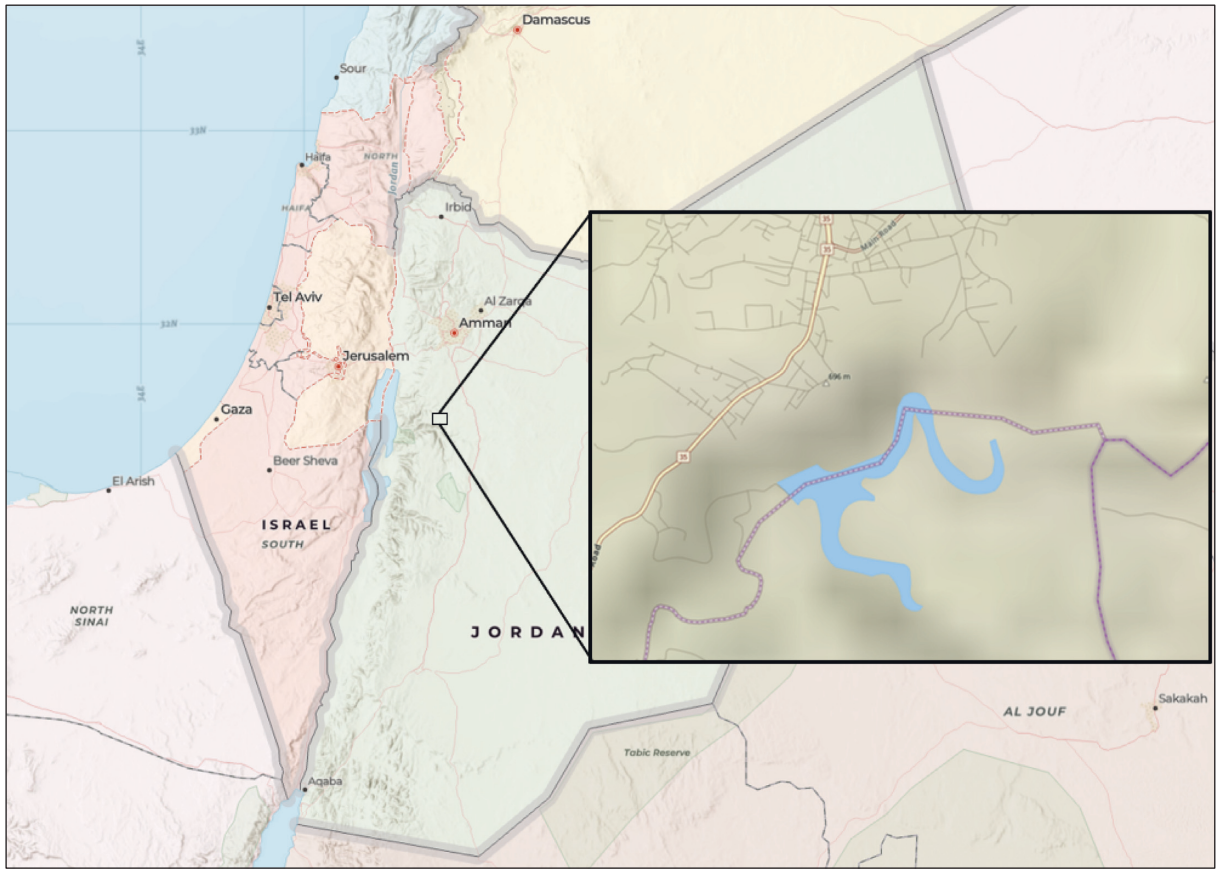

Figure 1: Wala dam location.

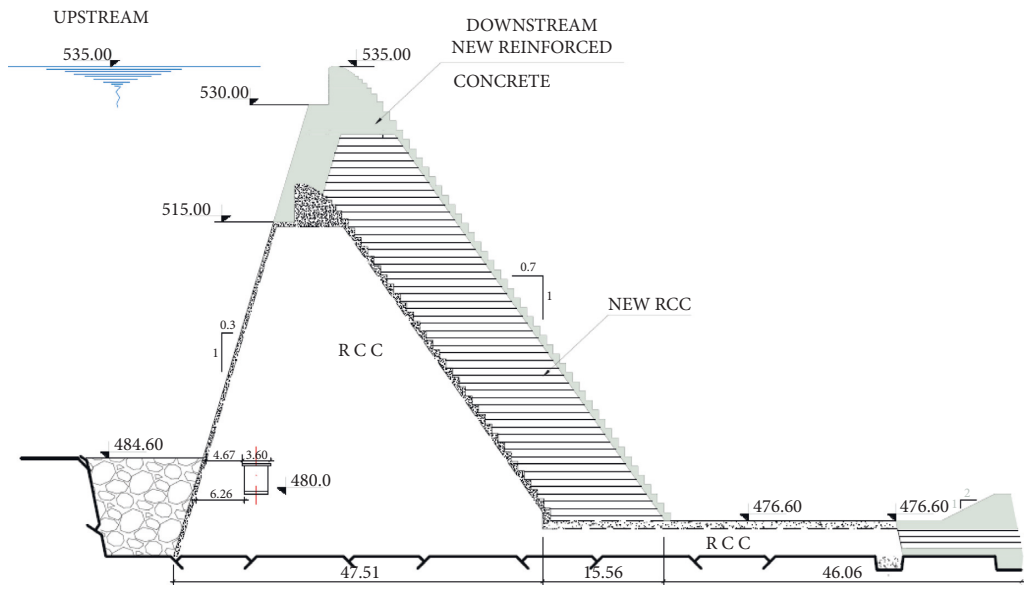

Figure 2: Cross-section of the main body of the Wala dam (original section and new raised section, after JVA, 2015a).

Since the foundation rock is infinite, the expanse of the foundation was considered to equal 100 m on each side of the dam, that is, to give an adequate representation of soil stiffness. The applied boundary conditions are taken so that no horizontal movement is allowed; thus, the foundation rock is restricted in all horizontal directions (i.e., there are rollers on vertical boundaries and at the bottom boundary). Therefore, the vertical direction movement is restricted in the bottom boundary as shown in Figure 6. Moreover, gravity loads due to the self-weight of both the rock

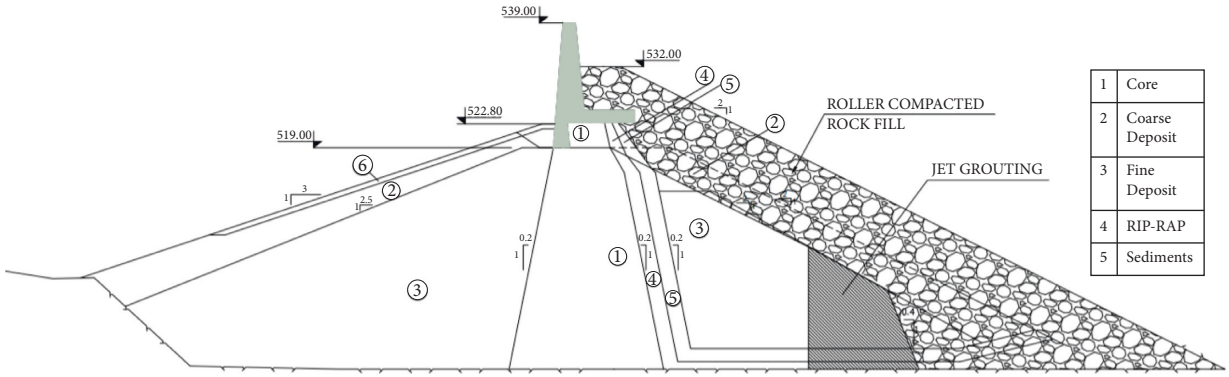

Figure 3: Raising of the wing embankment with reinforced concrete structure and roller-compacted rockfill part of Wala dam (after JVA, 2015a).

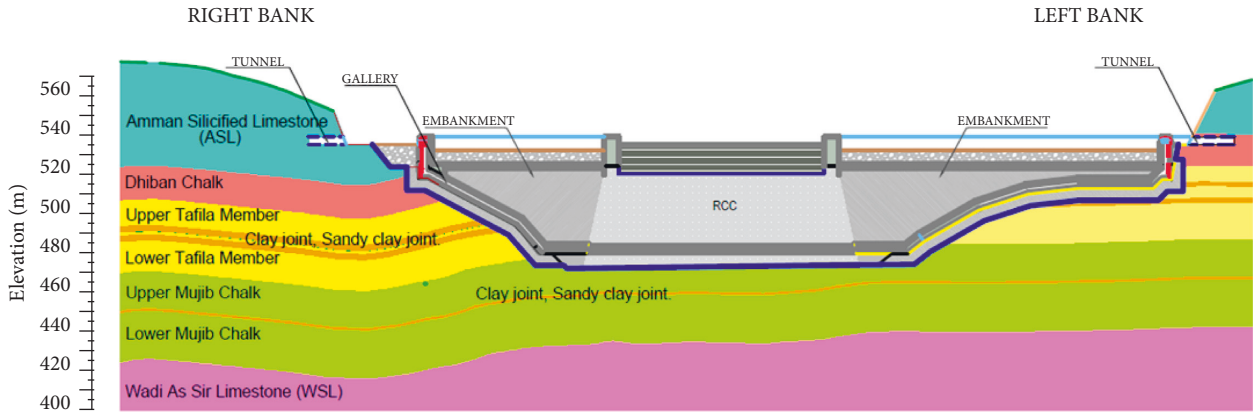

Figure 4: Geological cross-section of Wala dam site.

Table 1: Material soil properties of dam foundation and earthfill embankment.

Material	Elastic modulus, E (MPa)	Poisson's ratio, ν	Unit weight, γ (kN/m^3)	Friction angle, ϕ (°)
Core	200.0	0.35	20	25
Coarse deposit	170.0	0.25	22	35
Fine deposit	170.0	0.35	22	32
Filter	28.0	0.3	22	30
Drain	28.0	0.3	22	—
Riprap	170.0	0.25	23	45
Rockfill	170.0	0.25	23	45
Grouting curtain	—	0.25	22	45
Drainage curtain	—	0.25	22	—
Reinforced concrete	24,000.0	0.15	24	35
RCC	22,000.0	0.2	23	—
Foundation	17,000.0	0.2	20	35

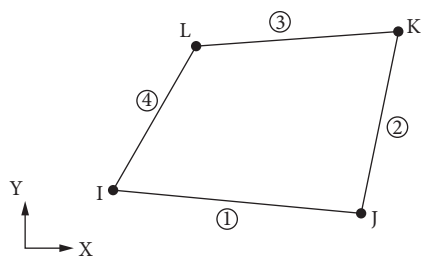

Figure 5: Finite element used in the analysis (PLANE182).

foundation and the dam were included in the material definition, while the hydrostatic pressure due to the weight of the water is replaced by nodal forces applied to the dam. Figures 7 and 8 show the finite element mesh for the two cross-sections of the dam (RCC section and dam foundation and earthfill embankment) for the initial and final sections.

The original RCC dam body section has a total number of elements and nodes equal to 675 and 1,468, respectively. Also, a total number of elements and nodes equal 1,537 and 3,274, respectively, for both the dam body and foundation

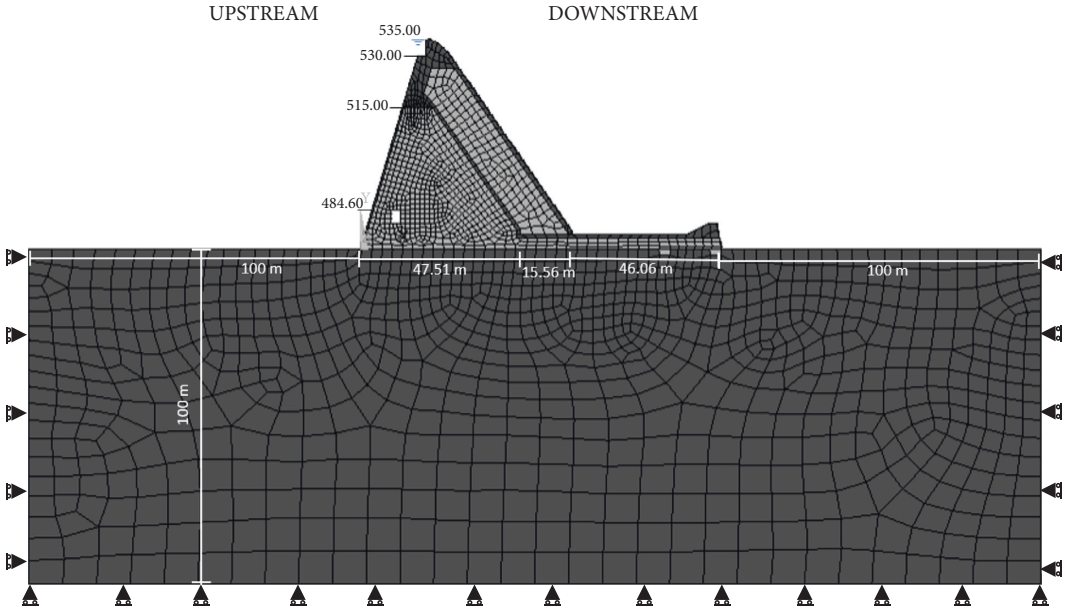

Figure 6: Dimensions and boundary conditions of the dam.

(Figure 7(a)), whereas the final RCC dam body section has a total number of elements and nodes equal to 896 and 1,928, respectively, and a total number of elements and nodes equal to 1,757 and 3,719 for both the dam body and foundation (Figure 7(b)).

On the other hand, for the dam foundation and earthfill embankment, the total number of elements and nodes for the initial dam body section are 1,054 and 2,266, respectively, and 2,147 and 4,634 for the dam and earthfill embankment (Figure 8(a)), while the final soil section has a total number of elements and nodes equal to 1,523 and 3,218, respectively, for the dam body and 2,616 and 5,566 for the dam and earthfill embankment (Figure 8(b)).

4. Result and Discussion

This section discusses the entire approach proposed in this study, with emphasis placed on the stresses' distribution and deformation in the dam's body and foundation as well as the earthfill embankment for the initial and final (raised wall) sections of the dam.

4.1. Stress Distribution in the RCC Section. The maximum principal stress distribution under the dam body for both the original dam and the newly raised dam is shown in Figure 9. Tensile stresses occurred at the upstream face of the dam for both sections (initial and final section). The values of the maximum tensile stress for the initial section and the final section were 0.65 MPa and 1.3 MPa, respectively, at the base of the dam. Additionally, the tensile zone for the initial section and the final section extended to about 12 m and 16 m, respectively. However, the downstream for both sections is basically in compression. On the other hand, the maximum principal stresses at the bottom level of the gallery showed minimal changes for both sections and can be neglected.

Figure 10 shows the contour of the maximum principal stresses on the upstream and downstream sides of the initial section and the final section. The stress difference between the two sections is considerably small and within acceptable limits (less than 1.5 MPa).

4.2. Stress Distribution in the Dam Foundation Soil and Earthfill Embankment. The maximum principal stress within the dam foundation soil and earthfill embankment for the initial and final sections are presented in Figure 11. The location where stresses were extracted and drawn is shown in Figure 11(a) (at the soil base and 18 m from the soil base). Referring to Figure 11(b), tensile and compression stresses are present at the dam soil foundations for the initial and final section. As seen, the tensile stresses have a maximum value of 0.2 MPa for the initial section and 0.48 MPa for the final section, even though the tensile stress of 0.48 MPa is considered a high value for the soil. However, no failure was observed within the soil. Moreover, the tensile zone is approximately the same for both sections, which extended to about 8 m. On the other hand, only compressive stresses were present for both sections at 18 m from the dam soil base as shown in Figure 11(c).

The contour of the maximum principal stresses of the dam foundation and earthfill embankment for the initial section and the final section is shown in Figure 12. Stresses in the downstream and upstream sides for the final section are greater than the stresses in the downstream and upstream sides of the initial section. However, the difference in stresses is considered insignificant and within an acceptable range.

4.3. Deformation of the Dam Body, the Dam Foundation, and Earthfill Embankment. The displacement distribution of the dam body and the soil of the Wala dam's new section is presented in Figure 13. Figure 13(a) shows the location

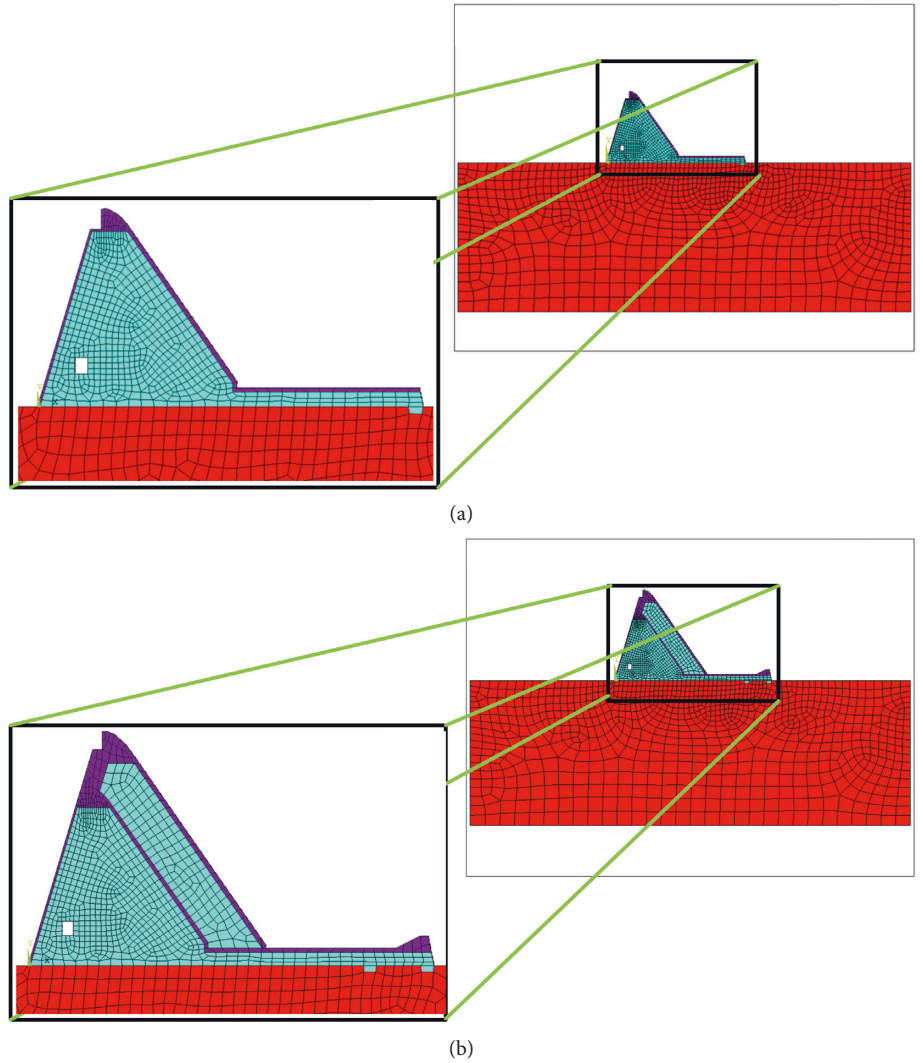

Figure 7: Finite element mesh of RCC section: (a) initial section and (b) final section.

where these displacement measurements were taken. Additionally, the maximum horizontal displacement and maximum vertical displacement occur at a distance of 55 m from the dam base as indicated by Figure 13(b), and the values are 0.09 m and 0.12 m, respectively.

Figure 14 shows the contour of the displacement of the dam foundation and earthfill embankment. It is clear that the maximum displacement occurs at the middle height of the downstream side and is approximately equal to 0.156 m. However, this displacement decreases rapidly toward the slopes of the dam (Figure 14(b)); the reduction of displacement from top to bottom is due to the action of the upper water load. Overall, the horizontal and vertical displacement at the end of construction have relatively small values, and this indicates the stable situation of the dam under these conditions.

Furthermore, stability analysis of slip surface of the new body of the dam structure using finite element method was analyzed. Two potential slip surfaces were examined, and a surface-to-surface contact element is modeled to simulate the slip surface. In problems containing contact between two bodies, one of the bodies is usually known as the "target or master" surface and the other as the "contact or salve" surface. For rigid-flexible contact, the target surface is always the rigid surface, and the contact surface is the deformable surface, which in this case represents the boundary in the new portion of the dam.

In the contact element, the relative motion in the interface produces the friction force (Ff). The basic Coulomb friction model for friction forces is indeterminate when two bodies are stuck; however, in reality, there is a small elastic deformation before the slip. The model is similar to the elasto-perfectly plastic model (see Figure 15).

The two contacting surfaces can carry shear stresses up to a certain magnitude across their boundary before they start sliding relative to each other. This state is known as sticking. The Coulomb friction model expresses equivalent shear stress (τ) when sliding on the boundary begins as a fraction of the contact normal pressure σn by the following equation:

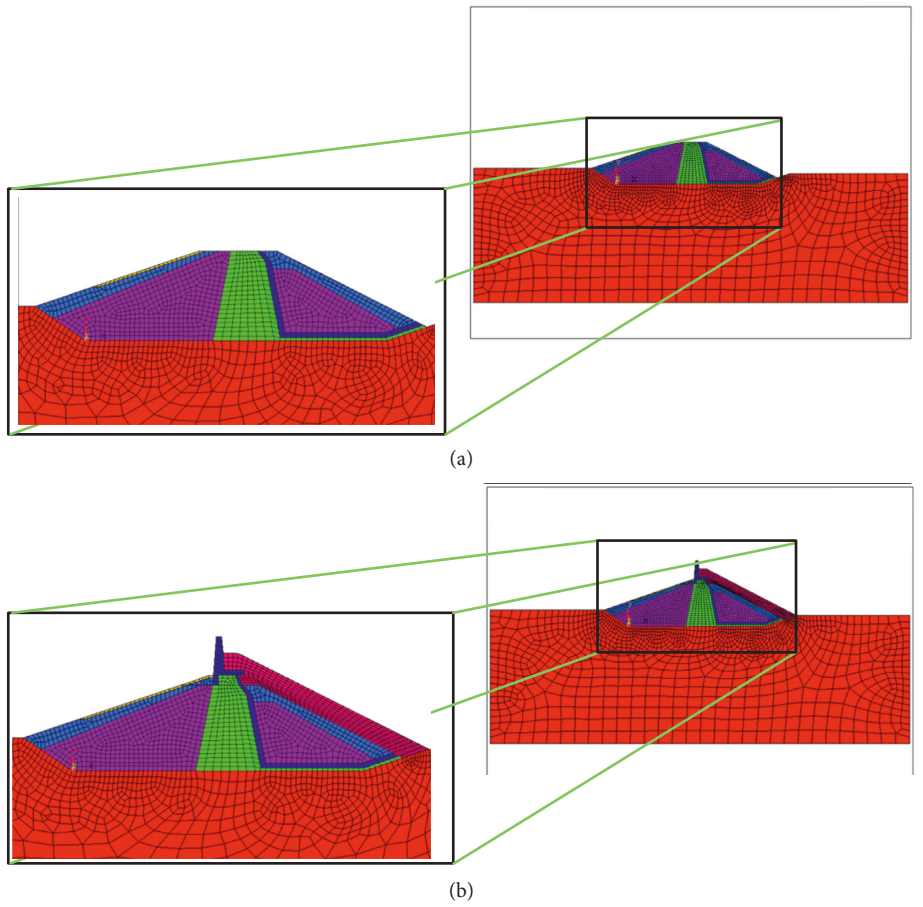

(a)

(b)

Figure 8: Finite element mesh of dam foundation and earthfill embankment: (a) initial section and (b) final section.

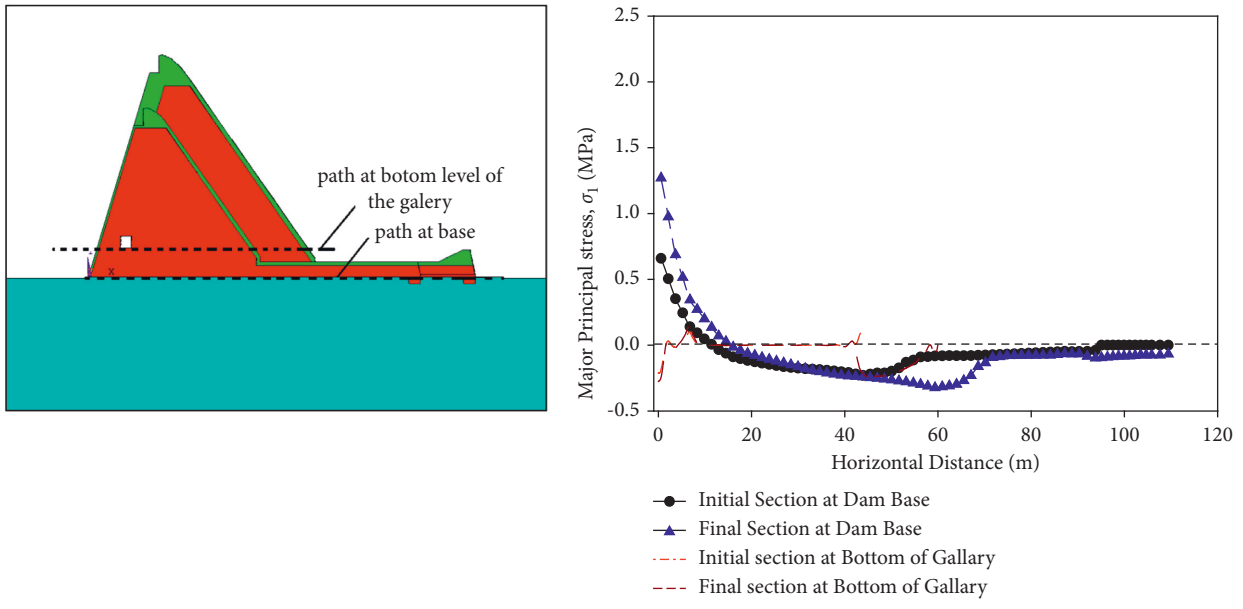

(a) (b)

Figure 9: Maximum principal stress distribution as a function of radial distance: (a) location where stresses were taken and (b) for initial and final section at the base of the dam body.

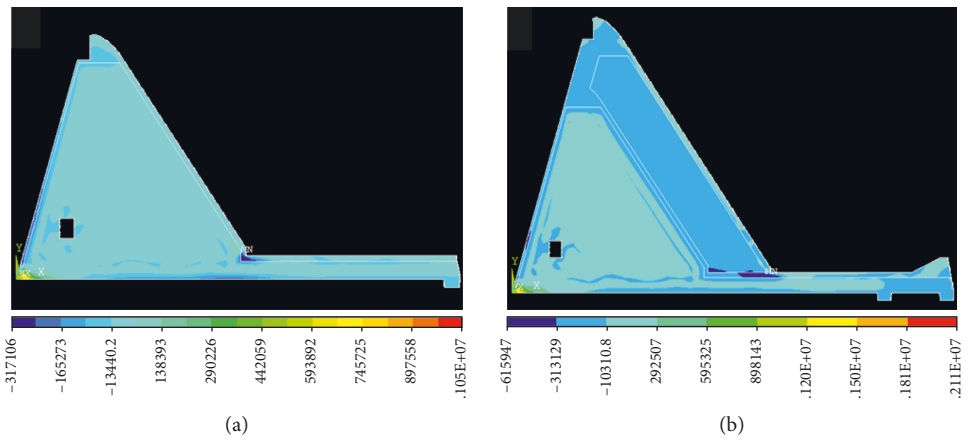

Figure 10: Contour of the maximum stresses of the dam body: (a) initial section and (b) final section.

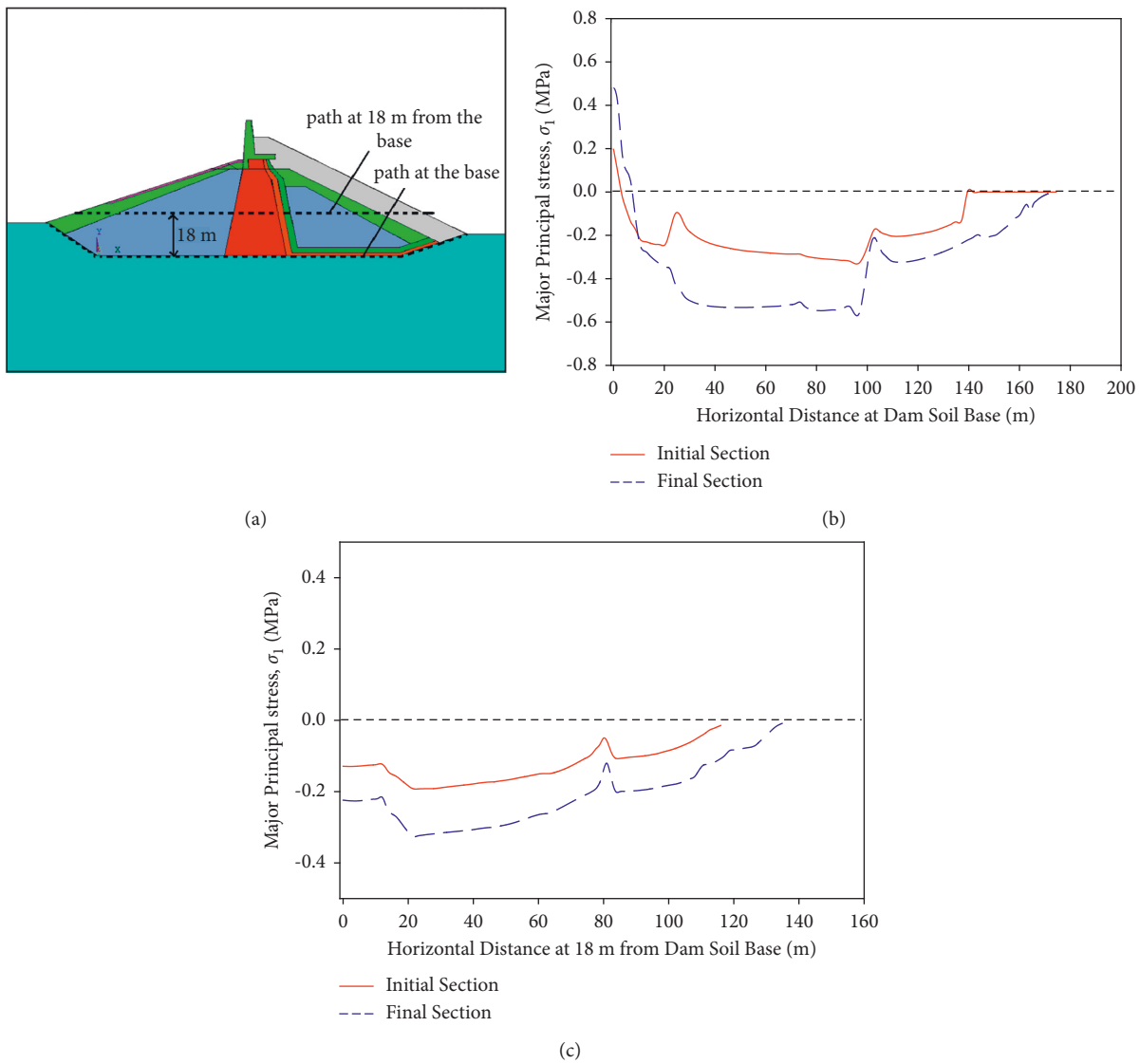

Figure 11: Maximum principal stress distribution as a function of radial distance: (a) location where stresses were taken, (b) for initial and final section at the dam foundation base and earthfill embankment, and (c) for initial and final section at 18 m from dam foundation and earthfill embankment base.

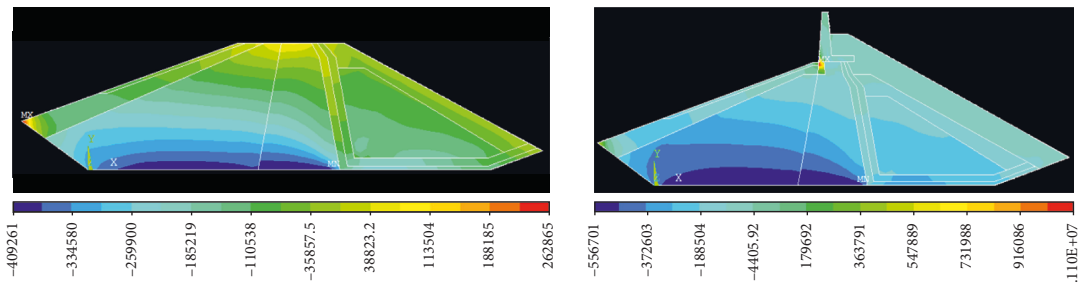

(a) (b)

Figure 12: Contour of the maximum principal stresses of the dam foundation and earthfill embankment: (a) initial section and (b) final section.

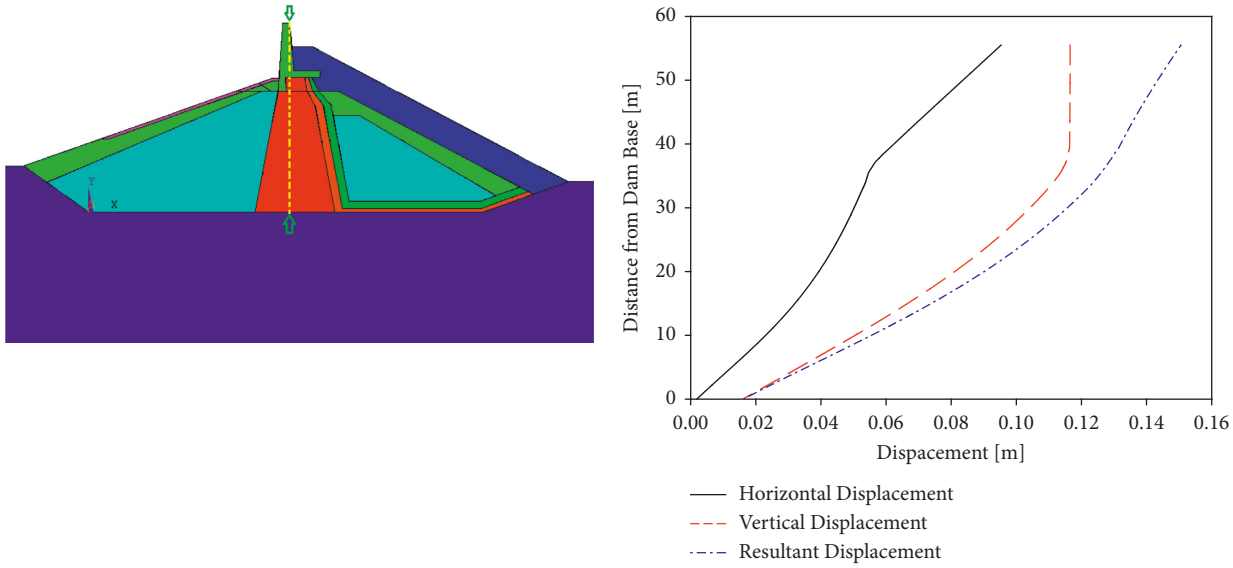

(a) (b)

Figure 13: Displacement distribution along the dam body: (a) where stresses were taken and (b) horizontal, vertical, and resultant displacement.

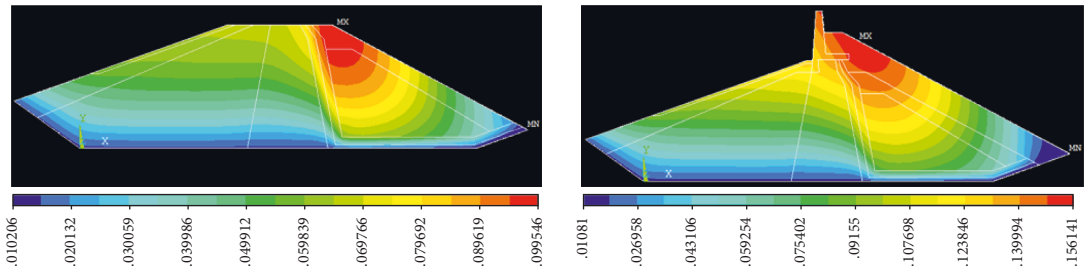

(a) (b)

Figure 14: Contour of displacement of the dam foundation and earthfill embankment: (a) initial section and (b) final section.

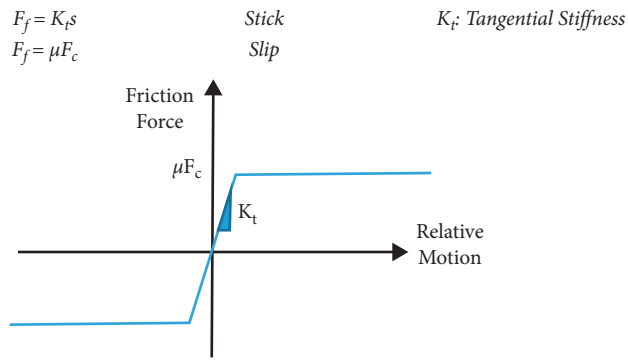

Figure 15: Elasto-perfectly plastic model.

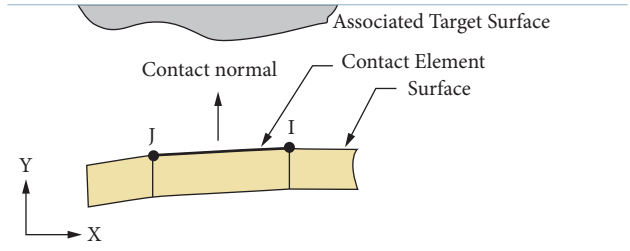

Figure 16: CONTA171 geometry (ANSYS manual).

$$\tau = \mu\sigma_n + C, \tag{1}$$

where $\mu$is the friction coefficient and C specifies the cohesion sliding resistance. Once the shear stress is exceeded, the two surfaces will slide relative to each other. This state is known as sliding. The sticking/sliding calculations determine when a point transitions from sticking to sliding, or vice versa.

ANSYS introduces several contact elements to model the contact surface. In this study, the CONTA171/TARGE169 pair elements (shown in Figure 16) are used between the old and new structures of the dam. The model can calculate the interface stresses as well as sliding distance. The calculated values are used to evaluate the stability state of the dam.

The type of contact element adopted for this study as discussed earlier is frictional contact where the two contacting geometries can carry shear stresses up to a certain magnitude across their interface before they start sliding relative to each other depending on the interface coefficient of friction, μ. This coefficient is used for the Coulomb friction that represents the ratio between the frictional force *Ff* and the normal R:

$$\tau = \mu R. \tag{2}$$

The analysis of the dam stability was carried out considering both water pressure (i.e., the reservoir is full of water) and earthquake loading. A peak ground acceleration of 0.20 g was considered in the analysis, which represents a return period of 475 years [28, 29].

Two cases were analyzed between the old and the new structure, case I (see Figure 17(a)) and case II (see Figure 17(b)). Only results of case II are presented and discussed here as they represent the more critical section. Case II shows that when friction coefficient μ increases the friction stress increases up to an ultimate value (0.3 MPa). Furthermore, when μ increases more than 0.3, the max friction stress decreases slightly then it stabilized (maybe due to the geometry of the structure) as shown in Figure 18(a). Additionally, results show that the sliding displacement is small (<0.02 m) for μ greater than 0.3, while, for $\mu < 0.2$, the sliding displacement increases rapidly causing the slop to fail (see Figure 18(b)). Finally, since the friction coefficient is generally much less than 0.3 MPa, thus, the factor of safety for sliding is high.

4.4. Comparison with Actual Displacement Measurement. Leveling survey devices and joint meters were placed at different locations of the dam wall to measure and monitor the settlement of the newly raised section of the Wala dam. For the surveying levels, monitoring started on the first day of June 2020, whereas the last measurement took place on September 7, 2021. While joint monitoring using joint meters started on December 23, 2020, the last reported reading was on August 10, 2021. Monitoring using surveying levels and joint meters will continue thereafter for both the right and left abutment. Figure 19 presents the different locations of the leveling surveys on the left and the right abutment. A total of 10 blocks (BR1–BR10) were used to monitor the right abutment and a total of 16 blocks (BL1–BL16) were used to monitor the left abutment; each block represents a level reading.

Figure 20 presents a time series of the monitored data for the left abutment; it can be concluded that during the first two months, almost no displacement occurred. However,

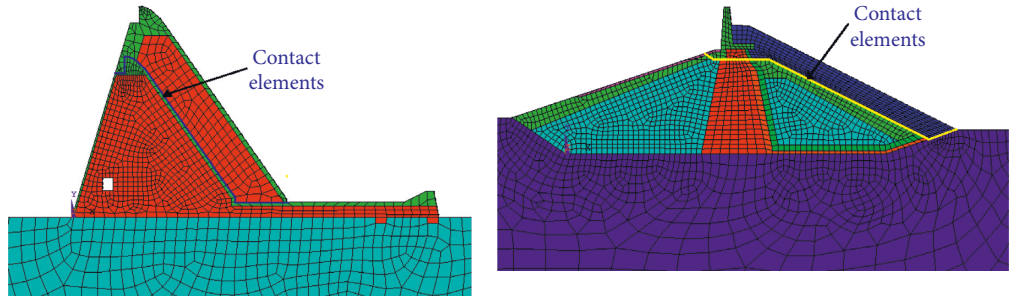

Figure 17: Critical sections analyzed: (a) concrete critical section and (b) soil critical section.

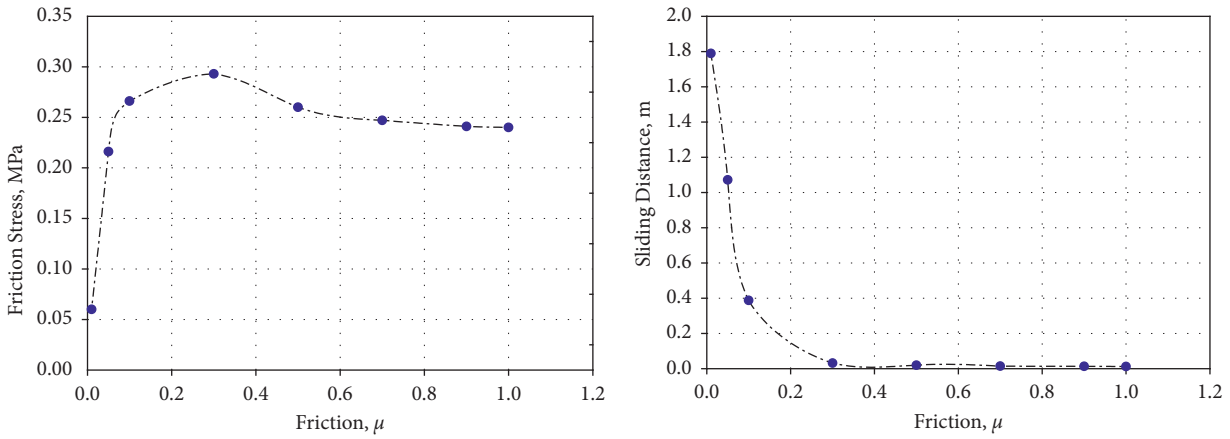

Figure 18: Effect of interface coefficient of friction between old and new section: (a) max shear frictional stress and (b) maximum sliding distance at interface layer.

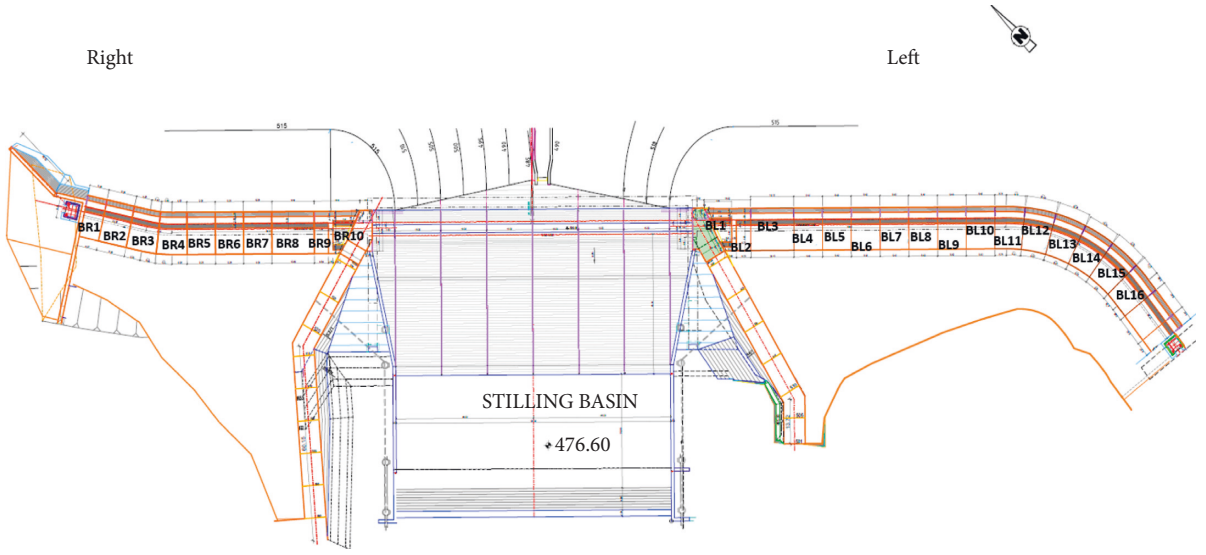

Figure 19: Location of leveling surveys at left and right abutment.

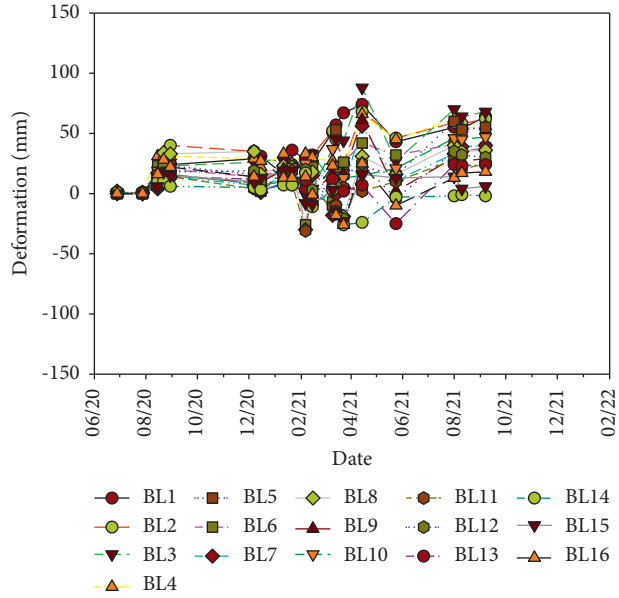

Figure 20: A time series of the change in deformation along the left abutment.

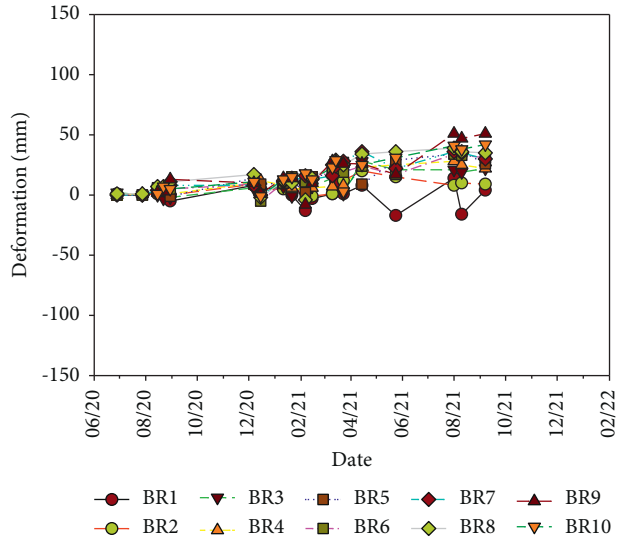

Figure 21: A time series of the change in deformation along the right abutment.

after the third month (August 2020) of monitoring (multiple readings were taken during August), the displacement increased in all blocks to a maximum value of approximately 0.04 m in block 2 (BL2). Furthermore, monitoring continued until September 2021; in April 2021 of that period, the displacement increased to a maximum value of 0.095 m in block 3 (BL3) and then slightly decreased in the following months. The last readings that were taken during September 2021 showed a maximum value that ranged between 0.062 and 0.068 m in blocks 1, 2, and 3 (BL1, BL2, and BL3).

Similarly, Figure 21 presents a time series of the monitored data for the right abutment; the data shows that minimum displacement occurred until February 2021. However, monitoring continued until September 2021; this displacement increased to a maximum value of approximately 0.029 m March 2021 in blocks 8 and 10 (BR8 and BR10). The last reading taken during September 2021 showed a maximum displacement value that ranged between 0.042 and 0.051 m in blocks 9 and 10 (BL9 and BL10).

It is worth mentioning that on January 27, 2021, the capacity of the reservoir was around 7 MCM and increased to around 10.8 MCM by February 6, 2021, yet the settlement readings during that period did not show any change on both abutments as shown in Figures 20 and 21. However, the JVA decided in early February (after February 6) as precautions to discharge around 200,000 m^3 every other day. Therefore, by February 17, 2021, the total discharge was around 1.2 MCM.

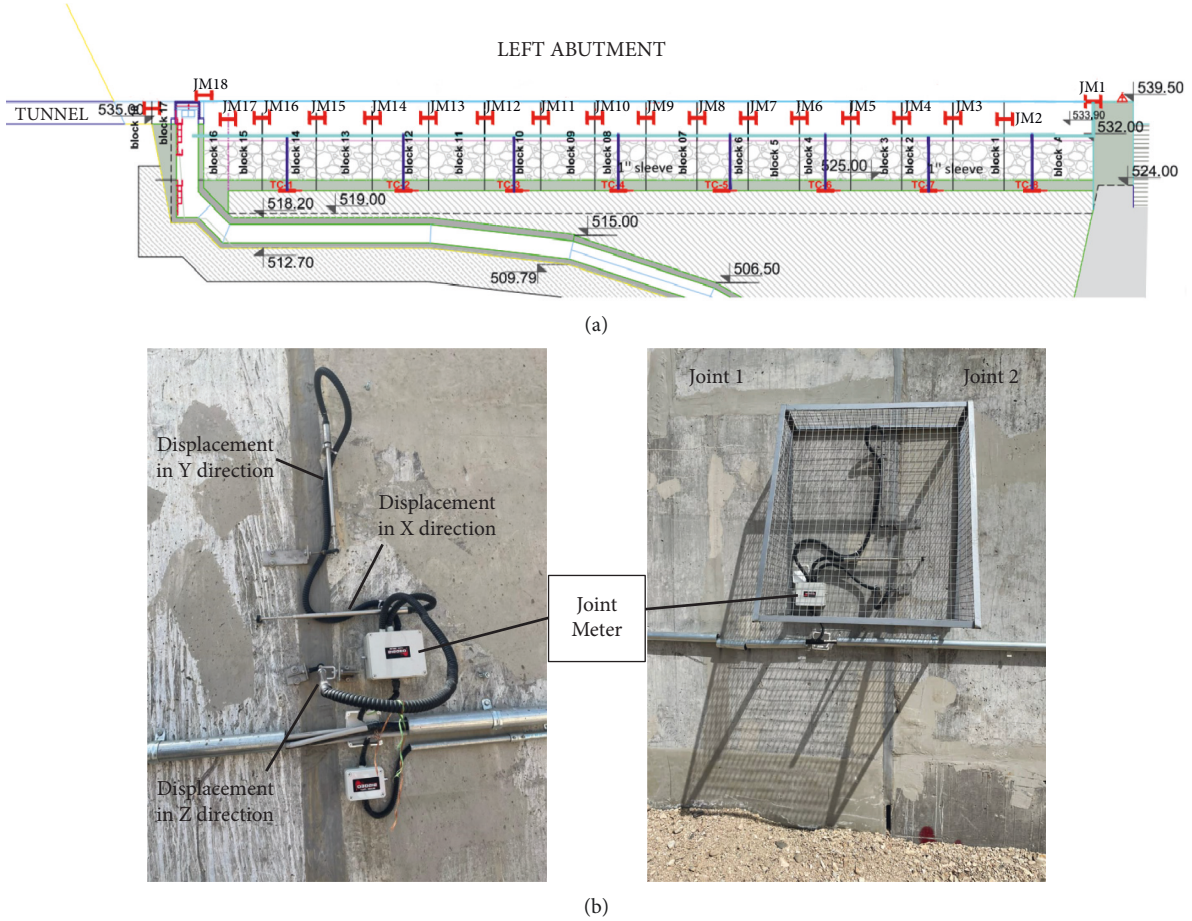

Figure 22: (a) Location of joint meters at left abutment and (b) photo of the joint meters.

The location of the joint meters for the left abutment is shown in Figure 22(a). The joint meters were used to monitor the movement of the joints (displacement) along the left abutment in three dimensions (X, Y, and Z); each joint meter was placed between two joints (Figure 22(b)). The displacement in the three directions is illustrated in Figure 23. For the x-direction (see Figure 23(a)), the movement was minimal in almost all 18 joint meters. However, the displacement in joint meter 1 (JM1) started to slightly change from February 1, 2021, and increased to a maximum value of ~0.004 m by February 28. Similarly, the movement of the joint meters in the Y and Z directions (Figures 23(b)and 23(c)) was minimal except for joint meter 1 (JM1), which started to show a slight change in displacement from February 1, 2021. Also, the maximum displacement reported on February 28, 2021, is ~0.0168 m and 0.024 m for the Y and Z directions, respectively. Thereafter, the displacement in the Y direction started to decrease, and the last reading that took place in August 2021 was ~0.011 m. However, the joint meter sensor in the Z direction stopped due to technical problems after March 2021. This change in displacement is reasonable as JM1 was resting on clay material. Also, the slight change in displacement could be attributed to the fact that the reservoir capacity was increased during that period as mentioned earlier. It is worth mentioning that joint meters were also placed at the right abutments, and almost no change in displacement was observed.

Interestingly, the conducted analysis revealed that there was no significant difference between the results obtained from this study and the data obtained from the fields. For instance, the finite element analysis showed that a maximum displacement of about 0.15 m occurred in the dam, while the field data using surveying levels showed an overall maximum displacement of about 0.095 m.

However, since the constructed concrete wall structure on the crest of the dam is of a unique design, attention should be paid to the possibility of internal erosion in the area of the joint (between the core and the concrete wall of the dam). Therefore, it is worth mentioning that measures should be taken to prevent the water from seeping under the constructed concrete wall, where no water will seep between the core and the concrete wall. Immediate measures should be taken by the JVA to make sure the water does not seep into the contact area between the constructed concrete wall and the core of the dam.

Taken together, these findings suggest that the results of the stability analysis of the newly constructed concrete wall show that the stresses and deformation are minimal and negligible.

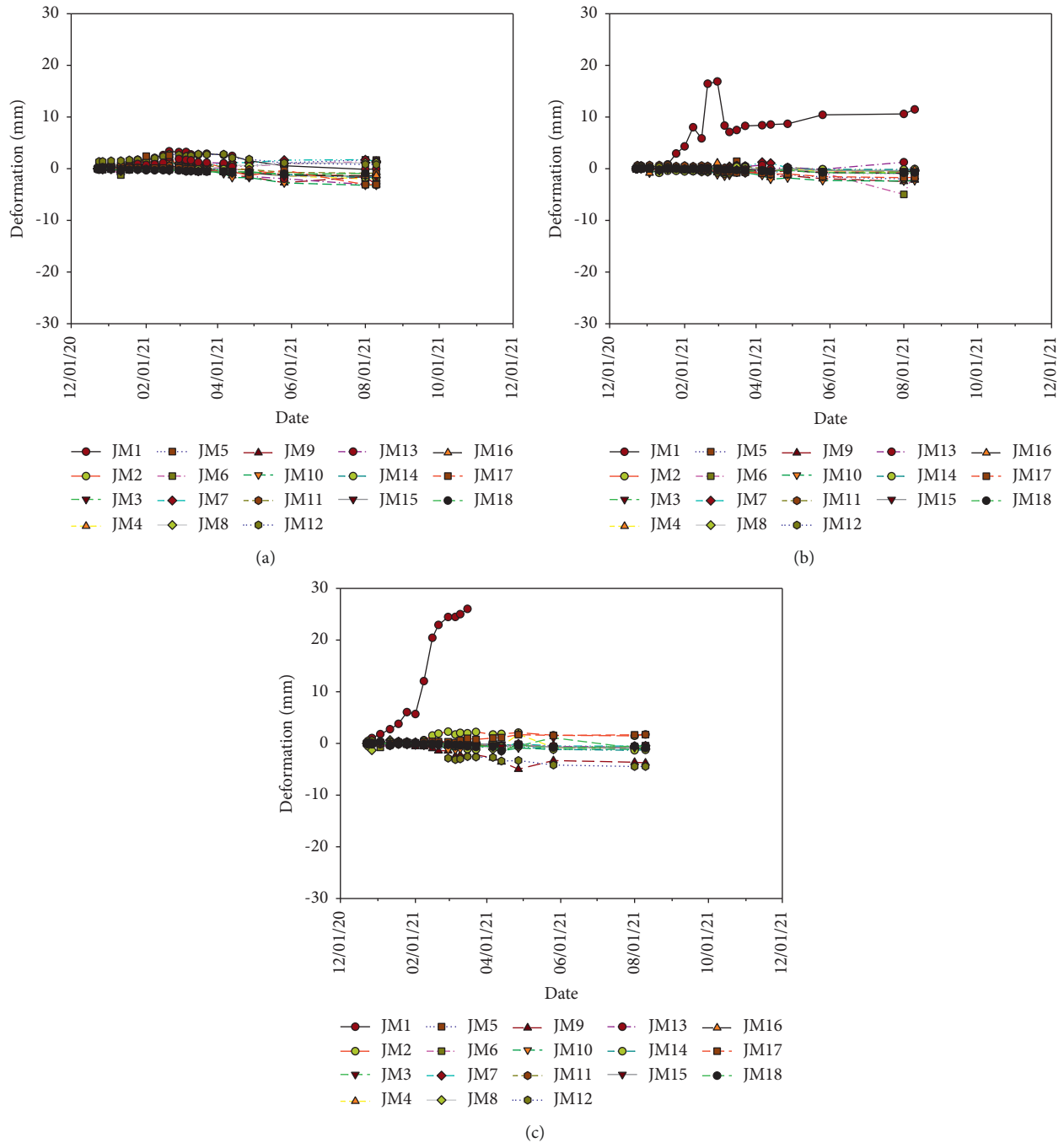

Figure 23: (a) Displacement measured in X direction, (b) displacement measured in Y direction, and (c) displacement measured in Z direction.

5. Conclusion, Recommendations, and Future Direction

Finite element analysis was conducted on the Wala dam to investigate the stability conditions after the height of the Wala dam is raised to increase its capacity. In this study, stresses and deformations of the new section within the dam body (RCC section) and soil foundation are presented and compared with the original dam. Based on the results, the following conclusions are drawn.

(i) The maximum tensile strength occurred at the upstream face of the dam body for both sections at the dam base and increased from 0.65 MPa to

1.3 MPa for the initial section and final section, respectively, while the downstream for both sections was in compression. Results from finite elements showed that the stresses after raising the height of the dam body are below 1.5 MPa. Therefore, the tensile strength is within the allowable range.

(ii) Tensile and compressive stresses were reported at the dam soil foundation for both sections. The tensile stress increased from 0.2 MPa to 0.48 MPa for the initial and final sections, respectively. Even though the tensile stress of the dam soil foundation increased to 0.48 MPa, no failure was observed or reported within the soil.

(iii) The tensile zone for the final section within the dam body increases by 33% when compared to the tensile zone for the initial section. While the tensile zone for the dam soil foundation was almost the same for both sections.

(iv) A maximum displacement of about 0.15 m occurred at a distance of 55 m from the dam base after raising the dam height. Also, higher displacement occurs at the middle height of the downstream face and decreases rapidly toward the slopes of the dam.

(v) Field monitoring of settlement of the new section of the Wala dam over a period of time (16 months) was conducted using surveying levels. During the first two months, both the left and right abutments did not show any settlement. However, after 10 months of monitoring the left abatement showed higher settlement than the right abutment. In addition, the right abutment showed minimal settlement, which is compatible with the finite element analysis results.

(vi) Joint meters were used to monitor joint movements in three dimensions (X, Y, and Z) along the left and right abutments. Higher displacement was observed at the left abutments compared to the right abutment, which is similar to that observation found using surveying levels. Generally, these movements along both abutments are minimal and show no risk to the dam stability.

(vii) The finite element analysis and the field monitoring results for the raised dam showed that the new raised dam enjoys stability and safety with acceptable stress and deformation design limits. Additionally, the stability analysis of the two potential slip surfaces of the new body of the dam structure shows (case II) that the factor of safety for sliding is high (much less than 0.3 MPa).

(viii) However, continuous field monitoring should be taken throughout the upcoming years, to monitor the behavior of the concrete wall to ensure the integrity of the dam.

(ix) The Jordan valley authority should consider and take prepositions to the possibility of internal erosion between the core and the constructed concrete wall.

In addition, the study shed light on the water agencies' guidelines and how these requirements can be updated to raise the dams' walls safely. Thus, this study provides the necessary knowledge about raising the dam's walls. As a result, it is recommended that MWI utilized the developed procedure to safely increase the dams' wall in order to increase the water capacity.

Due to practical constraints at the time of this study, further data collection is required. Future studies will verify the developed methodology with more field data and consider the rapid drawdown of water levels due to emergency conditions.

Data Availability

The data used to support the findings of this study are available from the corresponding author upon request.

Disclosure

The contents of this paper reflect the views of the authors and do not necessarily reflect the official views of the Ministry of Water and Irrigation/Jordan Valley Authority.

Conflicts of Interest

The authors declare that they have no conflicts of interest or personal relationships that could have appeared to influence the work reported in this paper.

Acknowledgments

This study was inspired by the Jordan Valley Authority, but the greatest impact comes from Eng. Hesham Al-Hesa, Director of Dams and Assistant Secretary-General of Jordan Valley Authority, and Prof. Khalil Belakhdar; their support, assistance in the analysis, and help are greatly acknowledged.

References

[1] M. Haddadin, "The socio-economic role of the king talal dam in the hashemite kingdom of Jordan," *Presentation at the World Commission on Dams Regional Consultation*, pp. 8-9, Cairo, Egypt, 1999.

[2] M. R. Maheri and M. Ranjbarzadeh, "Shape optimization of the new section in raising existing concrete gravity dams using genetic algorithm," *Dam Engineering*, vol. XX, no. 4, 2010.

[3] Ministry of Water and Irrigation, *Water for Life. Jordan's Water Strategy 2008–2022*", Ministry of Water and Irrigation of the Hashemite Kingdom of Jordan, Amman, Jordan, 2009.

[4] S. A. Barakat, A. I. H. Malkawi, and M. Omar, "Parametric study using FEM for the stability of the RCC Tannur dam," *Geotechnical & Geological Engineering*, vol. 23, no. 1, pp. 61–78, 2005.

[5] L. Ebner, S. Askelson, E. Thompson, and N. Cox, "Numerical modeling of the spillways for the dam raise at isabella dam," in *Proceedings of the Hydraulic Structures and Water System Management. 6th IAHR International Symposium on Hydraulic Structures*, pp. 498–507, Portland, OR, 2016 June.

[6] H. El Assad, B. Kissi, R. Hassan et al., "Numerical modeling of soil erosion with three wall laws at the soil-water interface," *Civil Engineering Journal*, vol. 7, no. 9, pp. 1546–1556, 2021.

[7] N. Hadadin, "Dams in Jordan current and future perspective," *Canadian Journal of Pure and Applied Sciences*, vol. 9, no. 1, pp. 3279–3290, 2015.

[8] B. A. Cherif, F. Ali, M. Tarek, and F. Massouh, "Mechanical behavior of the extraction mud dam for use in the manufacture of CEB," *Civil Engineering Journal*, vol. 7, no. 10, pp. 1774–1786, 2021.

[9] A. Toumi and B. Remini, "Evaluation of geology and hydrogeology of the water leakage in Hammam-Grouz Dam, Algeria," *Journal of Human, Earth, and Future*, vol. 2, no. 3, pp. 269–295, 2021.

[10] N. Kovacevic, P. R. Vaughan, and D. M. Potts, "Finite element analysis of ladybower dam: long-term operation and dam raising," in *Proceedings of the Long-term Behavior of Dams: Proceedings of the 2nd International Conference; LTBD09*, Graz, Austria, October 2009.

[11] G. Chavarri, A. De Fries, W. Y. Shieh, and C. H. Yeh, "Raising Guri gravity dam: stability and stress investigation," in *Proceedings of the Trans., 13th International Congress on Large Dams (ICOLD)*, pp. 45–56, New Delhi, India, June 1979.

[12] Ministry of Water and Irrigation/Jordan Valley Authority, *Policy and Adaptation in the Jordan Valley", Rosenberg International Forum V Managing Upland Watersheds in an Era of Global Climate Change Banff*, Canada, 2021.

[13] T. Uchida and T. Higashigawa, "A study on interface of new and old concrete with particular reference to raising of a gravity dam," in *Proceedings of the Trans., 13th International Congress on Large Dams (ICOLD)*, pp. 431–457, New Delhi, India, 1979 June.

[14] P. Tschernutter, S. Seiwald, and A. Kainrath, "Rheological behavior of an embankment dam after heightening," in *Proceedings of the 6th International Conference on Dam Engineering. LNEC*, pp. 1193–1219, Lisboa, July 2006.

[15] R. P. Brenner and S. Messerklinger, *The Challenger of Dam Heightening". International Symposium on Dams for a Changing World*, Kyoto, Japan, 2012.

[16] M. Y. Fattah, H. A. Omran, and M. A. Hassan, "Behavior of an earth dam during rapid drawdown of water in reservoir–case study," *International Journal of Advanced Research*, vol. 3, no. 10, pp. 110–122, 2015.

[17] M. Y. Fattah, S. N. Al-Labban, and F. A. Salman, "Seepage analysis of a zoned earth dam by finite elements," *International Journal of Civil Engineering & Technology*, vol. 5, no. 8, pp. 128–139, 2014.

[18] Y. Chen, L. Zhang, G. X. Yang, J. Dong, and J. Chen, "Anti-sliding stability of a gravity dam on complicated foundation with multiple structural planes," *International Journal of Rock Mechanics and Mining Sciences*, vol. 55, pp. 151–156, 2012.

[19] S. H. Liu, L. J. Wang, Z. J. Wang, and E. Bauer, "Numerical stress-deformation analysis of cut-off wall in clay-core rockfill dam on thick overburden," *Water Science and Engineering*, vol. 9, no. 3, pp. 219–226, 2016.

[20] F. Y. Chu, "Finite element analysis of stress deformation of earth-rock dam on narrow valley," *Applied Mechanics and Materials*, vol. 580, pp. 1852–1855, 2014.

[21] R. Wang and K. Yu, "Stress and deformation analysis of high concrete face rockfill dam based on COMSOL multiphysics IOP conference series: earth and environmental science," *IOP Conference Series: Earth and Environmental Science*, vol. 643, no. 1, Article ID 012013, 2021.

[22] A. I. Husein Malkawi and S. A. Mutasher, "A Direct Tensile Test for Roller Compacted Concrete (RCC) Gravity Dams," in *Proceedings of the 4th International Symposium on Roller Compacted Concrete (RCC) Dams*, Spain, 17-19 November 2003.

[23] A. A. Jawad, W. H. Hassan, and M. Y. Fattah, "Finite element analysis of a zoned earth dam under earthquake excitation IOP Conference Series: Material," *IOP Conference Series: Materials Science and Engineering*, vol. 1067, no. 1, Article ID 012074, 2021.

[24] S. Baluch and A. Chraibi, "Design and construction aspects of RCC works at Wala dam project, Jordan," in *Proceedings of the 2002 International Conference on Roller Compacted Concrete (RCC) Dam Construction in Middle East*, Jordan University of Science and Technology, Irbid, Jordan, April 2002.

[25] A. M. Abed, A. Darawiesh, and R. Naser, "Certain geological problems associated with RCC dams: case study for Wala and Mujib dams," in *Proceedings of the International Conference on Roller Compacted Concrete (RCC) Dam Construction in the Middle East*, Jordan University of Science and Technology, Irbid, Jordan, April 2002.

[26] Jordan Valley Authority, *Raising of Wala Dam, Design Report"*, Energoprojekt Hiroinzenjering Co. and Engicon Co. Volume B – Design Report, NY China, 2015.

[27] Jordan Valley Authority, *Raising of Wala Dam, Feasibility Study and Design Report"*, Energoprojekt Hiroinzenjering Co. and Engicon Co. Volume A – Summary Report, Bejing, 2015.

[28] M. J. Jiménez, *Jordan Seismic Hazard Mapping" Final Report 20.07.2004*, Institute of Earth Sciences "Jaume Almera" prepared for the Jordan Atomic Energy Commission (JAEC), Jorden, 2004.

[29] N. N. Ambraseys, K. A. Simpson, and J. J. Bommer, "Prediction of horizontal response spectra in Europe," *Earthquake Engineering & Structural Dynamics*, vol. 25, no. 4, pp. 371–400, 1996.